Research Square

Preprints are preliminary reports that have not undergone peer review.
They should not be considered conclusive, used to inform clinical practice,
or referenced by the media as validated information.

Sensitivity Analysis and Optimization of Burst Pressure in Composite Cylindrical Pressure Vessels

Saeed Abolghasemi

saeedabolghasemi2003@yahoo.com

Golestan University

Research Article

Keywords: burst pressure, composite pressure vessel, sensitivity analysis, design variables, failure criterion

Posted Date: July 30th, 2026

DOI: https://doi.org/10.21203/rs.3.rs-10479455/v1

License: This work is licensed under a Creative Commons Attribution 4.0 International License.
Read Full License

Additional Declarations: No competing interests reported.

Sensitivity Analysis and Optimization of Burst Pressure in Composite Cylindrical Pressure Vessels

Saeed Abolghasemi

Assistant Professor of Mechanical Engineering, Faculty of Engineering, Golestan University, Gorgan, Iran.

Email address: saeedabolghasemi2003@yahoo.com, s.abolghasemi@gu.ac.ir

Abstract

This paper presents a study on multivariable optimization of burst pressure in laminated composite cylindrical pressure vessels subjected to internal pressure. The stress analysis is based on the membrane theory of shells, and the burst pressure is estimated by the first-ply failure method. The fiber angle and individual layer thickness are considered as design variables in the optimization process. The sensitivities of the burst pressure with respect to the design variables are calculated analytically based on the Tsai–Hill and Tsai–Wu failure criteria. The optimal fiber angles, laminate thickness distributions, and the corresponding maximum burst pressure are determined for various symmetric and antisymmetric layups and subsequently compared. Furthermore, the through-thickness stress distributions corresponding to the optimum designs are evaluated and contrasted with those of non-optimal configurations. The results show that a significant improvement in the burst pressure of composite pressure vessels can be achieved through the appropriate selection of fiber orientation and layer thickness distribution.

Keywords: burst pressure; composite pressure vessel; sensitivity analysis; design variables; failure criterion.

1. Introduction

Composite materials are extensively used in the manufacturing of pressure vessels designed for the storage and transportation of industrial gases at elevated pressures. The excellent strength-to-weight ratio of composite pressure vessels enables significant weight reduction while maintaining the safety requirements associated with high-pressure gas containment. Burst pressure is the maximum internal pressure that a pressure vessel can withstand before the material strength is exceeded and structural integrity is lost. In laminated composite vessels, burst pressure depends on fiber orientation (winding angle),

number and thickness of layers, stacking sequence and material properties of fibers and matrix. Since the failure of a pressure vessel can have severe safety and economic consequences, ensuring structural integrity is a critical aspect of their design, material selection, and manufacturing processes. Consequently, the analysis and optimization of pressure vessels have attracted considerable attention from researchers and engineers over the past several decades.

Regassa et al. [1] used finite element analysis for stress and damage analysis of a composite overwrapped pressure vessel with a 4-mm-thick aluminum liner . Shen et al. [2] used a finite element model, developed in ANSYS to investigate the buckling behavior of filament-wound carbon-fiber-reinforced composite cylindrical shells subjected to external pressure under various boundary conditions. Das et al. [3] examined the influence of stacking sequence on the mechanical and thermomechanical properties of hybrid composites reinforced with both natural and synthetic fibers. Through dynamic mechanical analysis (DMA) and scanning electron microscopy (SEM), they demonstrated that the quantity and placement of glass fiber layers significantly affect the overall performance of hybrid laminates. Iwasaki et al. [4] proposed an iterative optimization methodology for composite pressure vessels with thin-walled elliptical heads based on a FE model of the vessel. Using Classical Laminate Theory (CLT) in conjunction with the Tsai–Wu failure criterion, they identified optimal stacking sequences that reduced the required laminate thickness while maximizing structural strength.

Neto et al. [5] investigated the burst behavior of composite pressure vessels subjected to internal pressure using the Tsai–Wu failure criterion, whereas the polymeric liner, consisting of a blend of high-density and low-density polyethylene, was analyzed based on the von Mises yield criterion. Chang [6] studied the first-ply failure strength of symmetrically laminated composite pressure vessels with different materials, geometrical configurations, and laminate thicknesses under uniform internal pressure. Wang et al. [7] proposed a progressive damage model for the failure analysis of aluminum/carbon-fiber/epoxy composite pressure vessels. They used finite element simulation in ABAQUS software for their analysis and compared their results with experimental data. Rafiee and Torabi [8] employed the first-ply failure (FPF) analysis based on various failure criteria to predict the burst pressure of composite pressure vessels by considering the effect of manufacturing uncertainties. Adali et al. [9] employed the membrane theory of shells to optimize the critical pressure of composite cylindrical vessels subjected to various loading conditions using the golden section method. Their work showed the effectiveness of optimization techniques in enhancing the load-carrying capability of composite pressure vessels. A similar approach was used by Chao et al. [10] to find the optimum fiber angle in symmetrically laminated cylinders. Azeem et al. [11] investigated the influence of fiber

winding angles on the hoop stress distribution in Type IV composite pressure vessels using finite element analysis and compared the performance of various winding configurations.

Islam et al. [12] investigated the stress behavior and burst performance of composite pressure vessels using finite element analysis, examining different fiber types and layup sequences to develop an optimal CPV configuration. Kang et al. [13] presented a hybrid optimization method for optimizing the winding angle and fiber volume fraction of a composite cylinder subjected to internal pressure, based on the Tsai–Wu failure criterion. The structural behavior of the cylinder was modeled using three-dimensional (3D) elasticity theory and the local sensitivities of the design variables were evaluated using the finite difference method. an analytical approach was presented by Matos et.al [14] to determine the optimum layup angle for maximizing the critical buckling pressure of thin composite cylinders that are subjected to external hydrostatic pressure. Onder et al. [15] studied the burst failure of filament-wound composite pressure vessels using analytical solution based on Lekhnitskii's theory, finite element, and experimental approaches. The burst pressure was evaluated for different winding angles and laminate configurations based on the Tsai–Wu, maximum stress, and maximum strain failure criteria. Their results indicated that a winding angle of 55° provides the highest burst pressure, while elevated temperatures reduce the vessel strength. Park and Sakai [16] developed a mathematical 3D elasticity solution for composite cylinders to optimize the fiber orientation through a global search algorithm that maximizes burst pressure under combined pressure, axial, and torsional loading conditions. Their results demonstrate the strong influence of stacking sequence and loading conditions on the burst performance of composite pressure vessels. A genetic algorithm-based optimization approach was presented in [17] for the design of composite cylinders under external hydrostatic pressure. Finite element analysis and the Tsai–Wu failure criterion was used to evaluate buckling and first-ply failure, respectively. The fiber orientations and laminate stacking sequence were optimized to maximize the allowable design pressure. The deformation and stress analysis of a thick composite cylinder reinforced with multi-angle filament winding under axial loading and internal/external pressure were performed by Xing et al. [18] using both analytical and finite element approaches. The results show the capability of multi-angle filament-wound pressure vessels to withstand higher pressures. Zhang et al. [19] proposed an analytical approach for burst pressure prediction and reliability analysis of composite overwrapped cylinders using the AFOSM method, where the layer thicknesses, spiral winding layer angles, and the internal pressure were considered as random variables. an analytical approach for the design and performance assessment of composite pressure vessels under combined internal pressure, axial loading, rotational effects, and hygrothermal environments was presented in [20]. Using classical lamination theory and several failure criteria, the authors evaluated optimum

winding angles, burst pressure, and maximum rotational speed. Mian et. al. [21] used finite element modeling for the design of lightweight composite pressure vessels. Based on Classical Lamination Theory and the Tsai–Wu failure criterion, the effects of material type, fiber orientation, and laminate stacking sequence on vessel performance were investigated. Liang et al.[22] adopted an efficient optimization method for the stacking sequence design of composite pressure vessels by joint application of finite element analysis (FEA), artificial neural networks (ANN), and genetic algorithms (GA). This method reduces the high computational cost of traditional optimization procedures by replacing repeated finite element evaluations with a trained neural network model. Santos et al. [23] used several machine-learning algorithms to predict the burst pressure of filament-wound composite pressure vessels and considered the effect of various process parameters such as fiber tension, winding speed, liner pressure, fiber volume fraction, winding time and curing pressure on the burst pressure.

In previous studies concerning design and optimization of composite pressure vessels, all layers of the laminated composite were typically assumed to have equal and constant thickness, and the influence of thickness distribution on the burst pressure, as well as its optimization potential, has received limited attention. In this paper, multivariable optimization of burst pressure in cylindrical composite vessels is attempted, in which the fiber angle and layer thickness are considered as design variables. Based on the Tsai–Hill and Tsai–Wu failure criteria, analytical sensitivity expressions for the burst pressure with respect to the design variables are derived. From the sensitivity analysis, the optimum configuration and the corresponding maximum burst pressure are calculated for various stacking sequences and are compared. The obtained results show that the pressure-carrying capacity of composite pressure vessels can be increased significantly by appropriate selection of fiber angles and laminate thickness distributions.

2. Problem formulation

2.1. Calculation of cylinder's burst pressure

In a thin-walled cylinder under internal pressure, the stress components according to the membrane theory of shells are given as:

$$\sigma_\theta = \frac{pr}{h}, \quad \sigma_L = \frac{pr}{2h} \tag{1}$$

Where σ_θ and σ_L are the hoop and axial stress components, respectively, p is the internal pressure, r is the radius of the cylinder and t is the wall thickness. As a result, any element of cylinder wall is subjected to a biaxial state of stress (Figure 1).

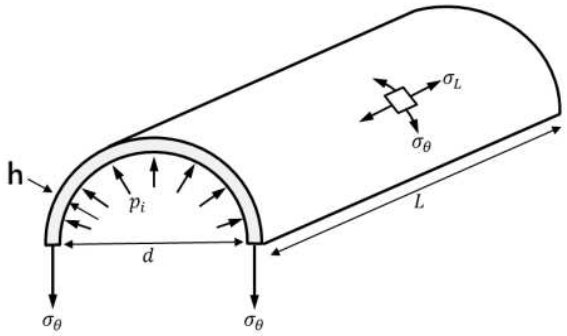


Figure 1. Axial and hoop stresses in a cylindrical vessel

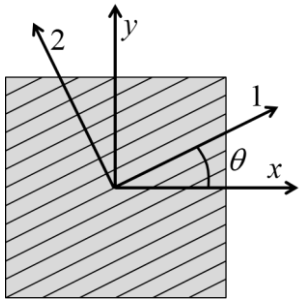


Figure 2. local and global coordinates of an angle lamina

The cylinder wall is composed of several orthotropic laminae stacked at different fiber orientations to form a laminate. The local (1-2) and global (x-y) coordinates which are used for analysis of a lamina, are shown in Figure 2. For an orthotropic lamina subjected to a plane-stress condition, the stress–strain relation in the local coordinates is given by [24]:

$$\begin{bmatrix}\sigma_1\\ \sigma_2\\ \tau_{12}\end{bmatrix}=\begin{bmatrix}\frac{E_1}{1-\nu_{12}\nu_{21}} & \frac{\nu_{12}E_2}{1-\nu_{12}\nu_{21}} & 0\\ \frac{\nu_{12}E_2}{1-\nu_{12}\nu_{21}} & \frac{E_1}{1-\nu_{12}\nu_{21}} & 0\\ 0 & 0 & G_{12}\end{bmatrix}\begin{bmatrix}\epsilon_1\\ \epsilon_2\\ \gamma_{12}\end{bmatrix} \quad (2)$$

The stress–strain relation in the global coordinate system is obtained through transformation as:

$$\begin{bmatrix}\sigma_x\\ \sigma_y\\ \tau_{xy}\end{bmatrix}=\begin{bmatrix}\overline{Q_{11}} & \overline{Q_{12}} & \overline{Q_{16}}\\ \overline{Q_{12}} & \overline{Q_{22}} & \overline{Q_{26}}\\ \overline{Q_{16}} & \overline{Q_{26}} & \overline{Q_{1661}}\end{bmatrix}\begin{bmatrix}\epsilon_x\\ \epsilon_y\\ \gamma_{xy}\end{bmatrix} \quad (3)$$

Where $\left[\overline{Q_{ij}}\right]$ is the reduced transformed stiffness matrix and is calculated as:

$$\left[\overline{Q_{ij}}\right]=[T]^{-1}[Q][R][T][R]^{-1} \quad (4)$$

Where $[R] = \begin{bmatrix} 1 & 0 & 0 \\ 0 & 1 & 0 \\ 0 & 0 & 2 \end{bmatrix}$ and the transformation matrix $[T]$ is defined as:

$$[T] = \begin{bmatrix} c^2 & s^2 & 2sc \\ s^2 & c^2 & -2sc \\ -sc & sc & c^2 - s^2 \end{bmatrix}, c = \cos(\theta), s = \sin(\theta) \tag{5}$$

The strain components are represented as:

$$\begin{bmatrix} \epsilon_x \\ \epsilon_y \\ \gamma_{xy} \end{bmatrix} = \begin{bmatrix} \dfrac{\partial u_0}{\partial x} \\ \dfrac{\partial v_0}{\partial y} \\ \dfrac{\partial u_0}{\partial y} + \dfrac{\partial v_0}{\partial x} \end{bmatrix} - z \begin{bmatrix} \dfrac{\partial^2 w_0}{\partial x^2} \\ \dfrac{\partial^2 w_0}{\partial xy^2} \\ 2\dfrac{\partial^2 w_0}{\partial x \partial y} \end{bmatrix} \tag{4}$$

Where u_0 , v_0 and w_0 are displacements of a point on the midplane. Eq. (4) can be rewritten as:

$$\begin{bmatrix} \epsilon_x \\ \epsilon_y \\ \gamma_{xy} \end{bmatrix} = \begin{bmatrix} \epsilon_{x0} \\ \epsilon_{y0} \\ \gamma_{xy0} \end{bmatrix} - z \begin{bmatrix} \kappa_x \\ \kappa_y \\ \kappa_{xy} \end{bmatrix} \tag{5}$$

Where κ_x, κ_y and κ_{xy} represent the bending and twisting curvatures of the laminate. Accordingly, the stress–strain relation in the global coordinate system can be expressed as:

$$\begin{bmatrix} \sigma_x \\ \sigma_y \\ \tau_{xy} \end{bmatrix} = \left[\overline{Q_{ij}}\right] \begin{bmatrix} \epsilon_{x_0} \\ \epsilon_{y_0} \\ \gamma_{xy_0} \end{bmatrix} - z\left[\overline{Q_{ij}}\right] \begin{bmatrix} \kappa_x \\ \kappa_y \\ \kappa_{xy} \end{bmatrix} \tag{6}$$

The force and moment resultants are defined as:

$$\begin{bmatrix} N_x \\ N_y \\ N_{xy} \end{bmatrix} = \int_{-h/2}^{h/2} \begin{bmatrix} \sigma_x \\ \sigma_y \\ \tau_{xy} \end{bmatrix} dz, \quad \begin{bmatrix} M_x \\ M_y \\ M_{xy} \end{bmatrix} = \int_{-h/2}^{h/2} \begin{bmatrix} \sigma_x \\ \sigma_y \\ \tau_{xy} \end{bmatrix} z dz \tag{7}$$

Now, by substituting Eq. (6) in (7), the force and moment resultants can be written in the following matrix form:

$$\begin{bmatrix} N \\ M \end{bmatrix} = \begin{bmatrix} A & B \\ B & D \end{bmatrix} \begin{bmatrix} \epsilon_0 \\ \kappa \end{bmatrix} \tag{8}$$

The extensional, bending-extension coupling and bending stiffness matrices are defined as

$$[A] = \sum_{k=1}^{n} \left[\overline{Q_{ij}}\right]_k (h_k - h_{k-1}); \; [B] = \frac{1}{2} \sum_{k=1}^{n} \left[\overline{Q_{ij}}\right]_k (h_k^2 - h_{k-1}^2); \; [D] = \frac{1}{3} \sum_{k=1}^{n} \left[\overline{Q_{ij}}\right]_k (h_k^3 - h_{k-1}^3) \tag{9}$$

Where h_k and h_{k-1} represent the z coordinates of the upper and lower surfaces of the *k*-th lamina, respectively (see Figure 3).

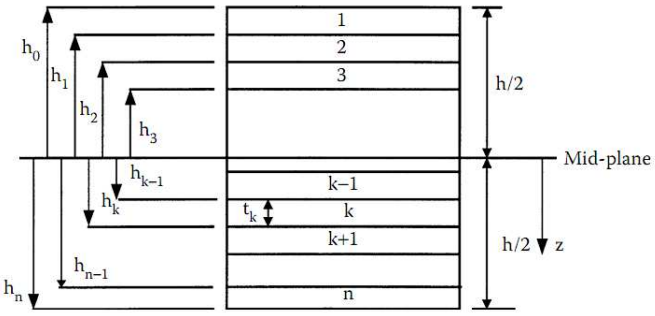


Figure 3. Coordinate of top and bottom surface of each lamina

Once the external loads acting on the laminate, namely the in-plane force (N) and moment (M) vectors, are specified, the mid-plane strains and curvature components can be determined from Eq. (8) as follows:

$$\begin{bmatrix}\epsilon_0\\ \kappa\end{bmatrix} = \begin{bmatrix}A & B\\ B & D\end{bmatrix}^{-1}\begin{bmatrix}N\\ M\end{bmatrix} \tag{10}$$

After obtaining the mid-plane strains and curvatures, the corresponding strain and stress distributions throughout the laminate thickness can be calculated from Eqs. (5) and (6), respectively. Afterwards, various failure criteria may be applied to estimate the burst pressure of the composite vessel. In this paper, both the Tsai-Hill and Tsai-Wu failure criteria are employed to predict and optimize the burst pressure of the composite cylinder. The Tsai-Hill theory is based on the distortion energy failure theory of von Mises for isotropic materials as applied to anisotropic materials. Based on this theory, the lamina will not fail if the following relation holds [10]:

$$\left(\frac{\sigma_1}{S_1^T}\right)^2 - \left(\frac{\sigma_1\sigma_2}{(S_1^T)^2}\right) + \left(\frac{\sigma_2}{S_2^T}\right)^2 + \left(\frac{\tau_{12}}{S_{12}}\right)^2 < 1 \tag{11}$$

Where σ_1, σ_2 and τ_{12} denote the stress components in local coordinate of the lamina, while S_1^T, S_2^T and S_{12} are the tensile and shear strengths of the lamina.

On the other hand, the Tsai–Wu criterion provides a more general failure theory by accounting for the interaction between different stress components. According to this criterion, a lamina is considered safe if the following condition is satisfied:

$$H_1\sigma_1 + H_2\sigma_2 + H_{11}\sigma_1^2 + H_{22}\sigma_2^2 + H_{66}\tau_{12}^2 + 2H_{12}\sigma_1\sigma_2 < 1 \tag{12}$$

Where the strength parameters are given as:

$$H_1 = \frac{1}{S_1^T} - \frac{1}{S_1^C};\ H_{11} = \frac{1}{S_1^T S_1^C};\ H_2 = \frac{1}{S_2^T} - \frac{1}{S_2^C};\ H_{22} = \frac{1}{S_2^T S_2^C};\ H_{66} = \frac{1}{S_{12}^2};\ H_{12} = -\frac{1}{2}\sqrt{H_{11}H_{22}} \tag{13}$$

To apply these criteria, the stress components must be first transformed from the global to the local coordinate of each lamina. This transformation is performed as follows:

$$\begin{bmatrix}\sigma_1\\ \sigma_2\\ \tau_{12}\end{bmatrix} = [T]\begin{bmatrix}\sigma_x\\ \sigma_y\\ \tau_{xy}\end{bmatrix} \tag{14}$$

Where the transformation matrix was defined in Eq. (5).

2.2. Sensitivity of burst pressure with respect to fiber angle

In this section, the analytical procedure for determining the sensitivity of burst pressure with respect to the fiber angle is described in detail for both failure criteria.

According to the Tsai-Hill criterion, the burst pressure can be calculated as:

$$p_{cr}^2\left(\left(\frac{\sigma_1}{S_1^T}\right)^2 - \left(\frac{\sigma_1\sigma_2}{(S_1^T)^2}\right) + \left(\frac{\sigma_2}{S_2^T}\right)^2 + \left(\frac{\tau_{12}}{S_{12}}\right)^2\right) = 1 \tag{15}$$

From which $p_{cr} = \sqrt{1/B}$, Where $B = \left(\frac{\sigma_1}{S_1^T}\right)^2 - \left(\frac{\sigma_1\sigma_2}{(S_1^T)^2}\right) + \left(\frac{\sigma_2}{S_2^T}\right)^2 + \left(\frac{\tau_{12}}{S_{12}}\right)^2$. To analyze the sensitivity of burst pressure with respect to fiber angle, the value of $\frac{\partial P_{cr}}{\partial\theta}$ is calculated from Eq. (15) as:

$$\frac{\partial P_{cr}}{\partial\theta} = -\frac{1}{2}\frac{\sqrt{B}}{B^2}\left(\frac{2\sigma_1\frac{\partial\sigma_1}{\partial\theta}}{S_1^{T^2}} - \frac{\left(\sigma_1\frac{\partial\sigma_2}{\partial\theta} + \sigma_2\frac{\partial\sigma_1}{\partial\theta}\right)}{S_1^{T^2}} + \frac{2\sigma_2\frac{\partial\sigma_2}{\partial\theta}}{S_2^{T^2}} + \frac{2\tau_{12}\frac{\partial\tau_{12}}{\partial\theta}}{S_{12}^2}\right) \tag{16}$$

The derivative of stress components in local coordinate can be calculated as:

$$\frac{\partial[\sigma_{12}]}{\partial\theta} = \frac{\partial[T]}{\partial\theta}[\sigma_{xy}] + [T]\frac{\partial[\sigma_{xy}]}{\partial\theta} \tag{17}$$

Where $[\sigma_{12}] = [\sigma_1, \sigma_2, \tau_{12}]^T$ and $[\sigma_{xy}] = [\sigma_x, \sigma_y, \tau_{xy}]^T$ represent the stress components in local and global coordinates, respectively. The value of $\partial[\sigma_{xy}]/\partial\theta$ appearing in Eq. (17) is calculated as:

$$\frac{\partial[\sigma_{xy}]}{\partial\theta} = \frac{\partial[\overline{Q_{ij}}]}{\partial\theta}[\epsilon_{xy}] + [\overline{Q_{ij}}]\frac{\partial[\epsilon_{xy}]}{\partial\theta} \tag{18}$$

Where $[\epsilon_{xy}] = [\epsilon_x, \epsilon_y, \epsilon_{xy}]^T$. Next, we should compute the derivative of strains with respect to fiber angle. To do this, we start with the relation $\begin{bmatrix}N\\ M\end{bmatrix} = \begin{bmatrix}A & B\\ B & D\end{bmatrix}\begin{bmatrix}\epsilon_0\\ \kappa\end{bmatrix}$ as was obtained in Eq. (8) and differentiate it w.r.t θ. The external loads applied to the composite vessel are constant and consequently, $\partial[N, M]^T/\partial\theta = 0$, which results:

$$\frac{\partial \begin{bmatrix} A & B \\ B & D \end{bmatrix}}{\partial \theta} \begin{bmatrix} \epsilon_0 \\ \kappa \end{bmatrix} + \begin{bmatrix} A & B \\ B & D \end{bmatrix} \frac{\partial \begin{bmatrix} \epsilon_0 \\ \kappa \end{bmatrix}}{\partial \theta} = 0 \tag{19}$$

From which the derivative of strains are computed as:

$$\frac{\partial \begin{bmatrix} \epsilon_0 \\ \kappa \end{bmatrix}}{\partial \theta} = - \begin{bmatrix} A & B \\ B & D \end{bmatrix}^{-1} \frac{\partial \begin{bmatrix} A & B \\ B & D \end{bmatrix}}{\partial \theta} \begin{bmatrix} \epsilon_0 \\ \kappa \end{bmatrix} \tag{20}$$

Eq. (20) can be written as a function of force and moment vector as:

$$\frac{\partial \begin{bmatrix} \epsilon_0 \\ \kappa \end{bmatrix}}{\partial \theta} = - \begin{bmatrix} A & B \\ B & D \end{bmatrix}^{-1} \frac{\partial \begin{bmatrix} A & B \\ B & D \end{bmatrix}}{\partial \theta} \begin{bmatrix} A & B \\ B & D \end{bmatrix}^{-1} \begin{bmatrix} N \\ M \end{bmatrix} \tag{21}$$

Where we have used the following expression for computing the derivative of the inverse of a matrix:

$$\frac{\partial \begin{bmatrix} A & B \\ B & D \end{bmatrix}^{-1}}{\partial \theta} = - \begin{bmatrix} A & B \\ B & D \end{bmatrix}^{-1} \frac{\partial \begin{bmatrix} A & B \\ B & D \end{bmatrix}}{\partial \theta} \begin{bmatrix} A & B \\ B & D \end{bmatrix}^{-1} \tag{22}$$

According to the definition of A, B and D matrices in Eq. (9), the value of $\frac{\partial \begin{bmatrix} A & B \\ B & D \end{bmatrix}}{\partial \theta}$ can be obtained as:

$$\frac{\partial [A]}{\partial \theta} = \sum_{k=1}^{n} \frac{\partial \left[\overline{Q_{ij}}\right]}{\partial \theta} (h_k - h_{k-1}); \quad \frac{\partial [B]}{\partial \theta} = \frac{1}{2} \sum_{k=1}^{n} \frac{\partial \left[\overline{Q_{ij}}\right]}{\partial \theta} (h_k^2 - h_{k-1}^2); \quad \frac{\partial [D]}{\partial \theta} = \frac{1}{3} \sum_{k=1}^{n} \frac{\partial \left[\overline{Q_{ij}}\right]}{\partial \theta} (h_k^3 - h_{k-1}^3) \tag{23}$$

Where $\frac{\partial \left[\overline{Q_{ij}}\right]}{\partial \theta}$ is obtained by differentiating Eq. (4) as:

$$\frac{\partial \left[\overline{Q_{ij}}\right]}{\partial \theta} = \frac{\partial [T]^{-1}}{\partial \theta} [Q][R][T][R]^{-1} + [T]^{-1}[Q][R] \frac{\partial [T]}{\partial \theta} [R]^{-1} \tag{24}$$

In the case of Tsai-Wu theory, the burst pressure can be calculated as:

$$P_{cr}(H_1\sigma_1 + H_2\sigma_2) + P_{cr}^2(H_{11}\sigma_1^2 + H_{22}\sigma_2^2 + H_{66}\tau_{12}^2 + 2H_{12}\sigma_1\sigma_2) = 1 \tag{25}$$

Eq. (25) can be written as a quadratic function of p_{cr} in the following form:

$$aP_{cr}^2 + bP_{cr} - 1 = 0 \tag{26}$$

Where

$$a = H_{11}\sigma_1^2 + H_{22}\sigma_2^2 + H_{66}\tau_{12}^2 + 2H_{12}\sigma_1\sigma_2, \quad b = H_1\sigma_1 + H_2\sigma_2 + H_6\tau_{12} \tag{27}$$

This quadratic equation yields a negative and a positive root, and the positive root is taken as the burst pressure. To calculate the sensitivity in this case, equation (26) must be differentiated as:

$$\frac{\partial a}{\partial \theta}P_{cr}^2 + 2aP_{cr}\frac{\partial P_{cr}}{\partial \theta} + \frac{\partial b}{\partial \theta}P_{cr} + b\frac{\partial P_{cr}}{\partial \theta} = 0. \tag{28}$$

Solving the above equation for $\frac{\partial P_{cr}}{\partial \theta}$ results in:

$$\frac{\partial P_{cr}}{\partial \theta} = -\frac{P_{cr}\left(\frac{\partial a}{\partial \theta}P_{cr} + \frac{\partial b}{\partial \theta}\right)}{2aP_{cr} + b} \tag{29}$$

2.3. Sensitivity of burst pressure with respect to layer thickness

A similar procedure is used to calculate the variation of burst pressure with respect to the thickness of the *i-th* layer, t_i. In this case, the terms $\frac{\partial(.)}{\partial \theta}$ appearing in Eqs. (16) and (29) must be replaced by $\frac{\partial(.)}{\partial t_i}$. Since the transformation matrix $[T]$ and the reduced transformed stiffness matrix $\left[\overline{Q_{ij}}\right]$ are independent of t_i, only the derivatives of the laminate stiffness matrices A, B, and D with respect to $t_i$need to be evaluated as follows:

$$\begin{aligned}
\frac{\partial [A]}{\partial t_i} &= \sum_{k=1}^{n}\left[\overline{Q_{ij}}\right]\left(\frac{\partial h_k}{\partial t_i} - \frac{\partial h_{k-1}}{\partial t_i}\right); \\
\frac{\partial [B]}{\partial t_i} &= \sum_{k=1}^{n}\left[\overline{Q_{ij}}\right]\left(h_k\frac{\partial h_k}{\partial t_i} - h_{k-1}\frac{\partial h_{k-1}}{\partial t_i}\right) \\
\frac{\partial [D]}{\partial t_i} &= \sum_{k=1}^{n}\left[\overline{Q_{ij}}\right]\left(h_k^2\frac{\partial h_k}{\partial t_i} - h_{k-1}^2\frac{\partial h_{k-1}}{\partial t_i}\right)
\end{aligned} \tag{30}$$

Where $h_k = -\frac{h}{2} + \sum_{i=1}^{k-1} t_k \ , k = 1,2,\dots,n$ represents the coordinate of top surface of layer k. To facilitate the numerical calculation of the derivatives $\frac{\partial h_k}{\partial t_i}$ in programming, a simple Jacobian matrix is defined as:

$$J = \begin{bmatrix}
\frac{\partial h_1}{\partial t_1} & \frac{\partial h_1}{\partial t_2} & \frac{\partial h_1}{\partial t_3} & \cdots & \frac{\partial h_1}{\partial t_k} \\
\frac{\partial h_2}{\partial t_1} & \frac{\partial h_2}{\partial t_2} & \frac{\partial h_2}{\partial t_3} & & \\
\frac{\partial h_3}{\partial t_1} & & & & \\
 & & & & \\
\frac{\partial h_{k+1}}{\partial t_1} & & & & \frac{\partial h_{k+1}}{\partial t_k}
\end{bmatrix} \tag{31}$$

Following the same procedure as was described in Eq. (20), the derivatives of the mid-plane strains and curvatures can be expressed as:

$$\frac{\partial \begin{bmatrix} \epsilon_0 \\ \kappa \end{bmatrix}}{\partial t_i} = -\begin{bmatrix} A & B \\ B & D \end{bmatrix}^{-1} \frac{\partial \begin{bmatrix} A & B \\ B & D \end{bmatrix}}{\partial t_i} \begin{bmatrix} \epsilon_0 \\ \kappa \end{bmatrix} \tag{32}$$

since $[\epsilon] = [\epsilon_0] - z[\kappa]$, (see Eq. (5)), the variation of strain components at top and bottom surface of each layer is computed as:

$$\frac{\partial [\epsilon]_k}{\partial t_i} = \frac{\partial [\epsilon_0]}{\partial t_i} - z_k \frac{\partial [\kappa]}{\partial t_i} - \frac{\partial z_k}{\partial t_i} [\kappa] \tag{33}$$

Note that at the top and bottom surfaces of composite layers, we have $z_k = h_k$, where the value of h_k was defined as $h_k = -\frac{h}{2} + \sum_{i=1}^{k-1} t_k \ , k = 1,2, \dots, n$. Now the variation of global stress components for each layer can be calculated as:

$$[\sigma_{xy}]_k = [\overline{Q_{ij}}]_k [\epsilon_{xy}]_k \rightarrow \frac{\partial [\sigma_{xy}]_k}{\partial t_i} = [\overline{Q_{ij}}]_k \frac{\partial [\epsilon]_k}{\partial t_i} \tag{34}$$

And finally, the variation of local stress components is calculated as:

$$\frac{\partial [\sigma_{12}]_k}{\partial t_i} = [T] \frac{\partial [\sigma_{xy}]_k}{\partial t_i} \tag{35}$$

2.4. Optimization procedure

A cylindrical pressure vessel with closed ends subjected to an internal pressure p is considered. The objective is to determine the fiber angle θ and the layer thicknesses $t_i, i = 1,2, .., n$, (see Figure 3) which maximizes the burst pressure of the composite cylinder against a failure criterion. The burst pressure is calculated according to the First-Ply Failure (FPF) method. In this approach, the critical pressure corresponding to each surface of every lamina is evaluated based on the selected failure criterion. The burst pressure of the composite vessel is then defined as the minimum of these critical pressures, representing the pressure at which the first ply fails, i.e. $P_{cr} = \min_k P_{cr}^{(k)}$. The design optimization problem is defined as:

$$\begin{aligned} P_{\max} &\overset{def}{=} \max P_{cr}(X) = \max \min_k p_{cr}^{(k)} \\ &subject\ to: \sum_{k=1}^{n} t_k = h \end{aligned} \tag{36}$$

Where $X = [\theta, t_1, t_2, \dots, t_n]^T$ is the vector of design variables and h is the total wall thickness of the vessel and is assumed to be constant. A gradient-based optimization procedure is implemented in MATLAB for finding the optimum value of burst pressure by utilizing the sensitivities of the objective function with respect to the design variables, which were

calculated at the previous section. We start with an initial guess of design variables. Then, structural analysis is first performed to evaluate the objective function. Next, sensitivity analysis is carried out to determine the derivatives of the objective function with respect to the design variables, which show the rate and direction of change of the response due to small variations in the design parameters. This procedure is continued until a convergence criterion is satisfied.

3. Results and discussion

This section presents numerical results for optimization of burst pressure in composite cylindrical vessels for various stacking sequences and two composite materials. The optimal design variables and the corresponding maximum burst pressures are determined using two failure criteria, namely the Tsai–Hill and Tsai–Wu theories.

3.1. Validation study

To verify the validity of the proposed solution procedure and the accuracy of the calculations, the results are compared with those reported by Adali et.al. [9], where the burst pressure of a composite cylinder with four- and six-layer symmetric laminates is presented in Figure 4. As can be seen, the predicted critical pressures are in good agreement with the reference results, demonstrating the accuracy and reliability of the proposed approach for analyzing composite cylinders. The laminate which was used in this validation study is made of T300/5208 graphite/ epoxy, the elastic constants of which are:

$E_1 = 142\ \ GPa, E_2 = 10.8\, GPa, G_{12}\ = 5.49\ \ GPa, v_{12} = 0.3$. The strength values are $X_t = 1568\, MPa, X_c = 1341\ \ MPa, Y_t\ = 57\ \ MPa, Yc = 212\ \ MPa, S = 80\ \ MPa.$

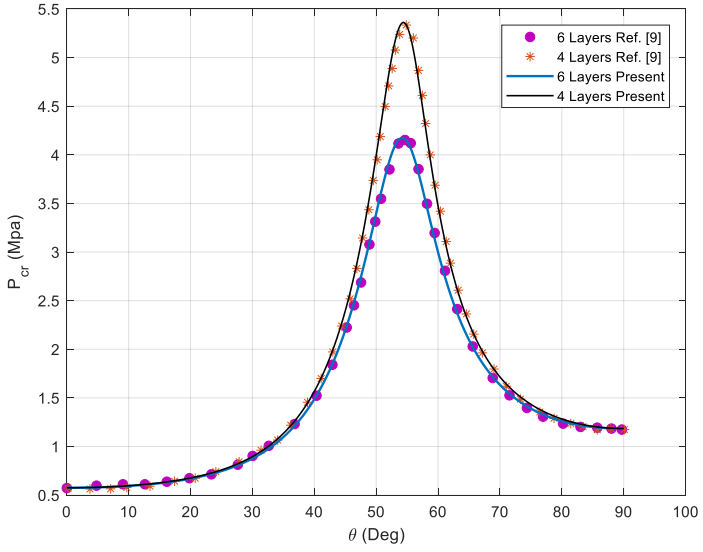


Figure 4. Comparison of burst pressure of symmetric composite cylinders with the results of Ref. [9].

3.2. Optimization of fiber angle

Based on the sensitivity analysis developed in the previous sections, the results for optimization of the fiber angle to achieve maximum burst pressure are presented in Table 1 for various stacking sequences. In this analysis, the layer thicknesses are assumed to be uniform and given by $t_i = h/n$, where h is total thickness and n is the number of layers. Two types of composite laminates, namely Glass/epoxy and Graphite/epoxy, are considered in this study. The mechanical properties of these laminates are summarized in Table 2.

Table 1. Optimum fiber angle and the corresponding burst pressure of a composite cylinder.

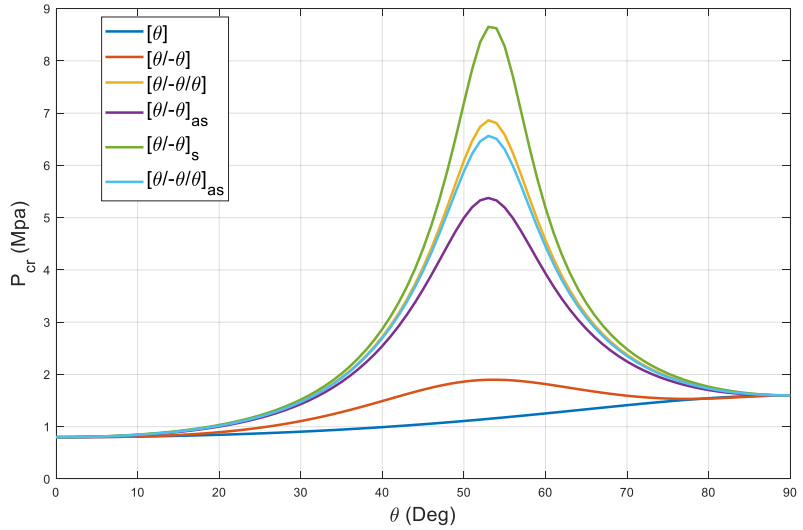
Material	graphite-epoxy				Glass-epoxy			
Failure criterion	Tsai-Hill		Tsai-Wu		Tsai-Hill		Tsai-Wu	
Lay-up	θ°_{opt}	$P_{cr}\ (Mpa)$	θ°_{opt}	$P_{cr}\ (Mpa)$	θ°_{opt}	$P_{cr}\ (Mpa)$	θ°_{opt}	$P_{cr}\ (Mpa)$
$[\theta]$	90.00	1.60	90.00	1.63	90.00	1.24	90.00	1.32
$[\theta/-\theta]$	53.67	1.90	54.37	1.82	90.00	1.24	90.00	1.32
$[\theta/-\theta/\theta]$	53.20	6.87	54.06	6.99	54.14	1.94	54.63	2.13
$[\theta/-\theta]_{as}$	52.99	5.38	53.85	5.32	54.84	1.60	55.35	1.68
$[\theta/-\theta]_{s}$	53.42	8.68	54.20	8.92	53.69	2.37	54.22	2.72
$[\theta/-\theta/\theta]_{as}$	53.16	6.57	54.02	6.60	54.19	1.84	54.68	1.98
$[\theta/-\theta/\theta]_{s}$	53.20	6.87	54.06	6.99	54.14	1.94	54.63	2.13
$[\theta/-\theta/0/\theta/-\theta]$	61.46	6.35	62.71	6.48	90.00	1.96	90.00	2.21
$[\theta/-\theta/0/-\theta/\theta]$	68.49	7.50	68.49	8.05	81.18	2.02	81.18	2.29
$[\theta/0/-\theta]$	90.00	7.47	90.00	8.01	90.00	1.90	90.00	2.09

Table 2. Mechanical properties of Glass/epoxy and Graphite/epoxy laminates [24].

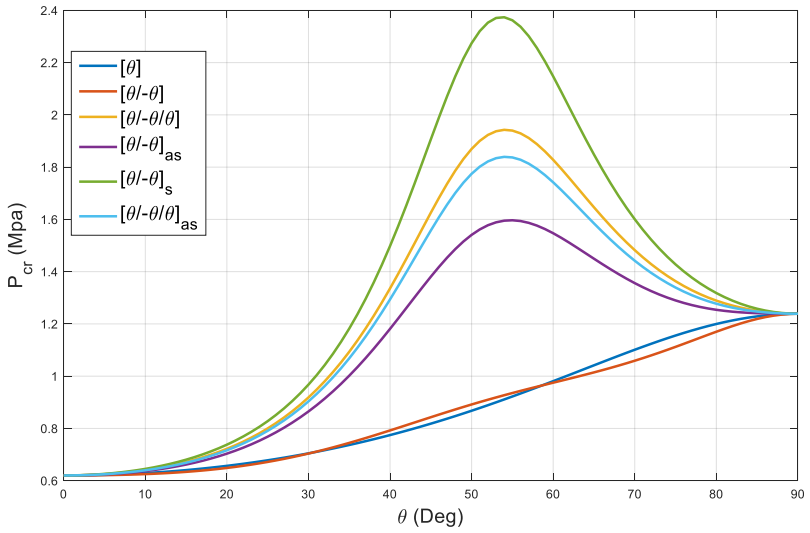
Property	Laminate	
	Glass/epoxy	Graphite/epoxy
$E_1(Gpa)$	38.6	181
$E_2(Gpa)$	8.27	10.38
ν_{12}	0.26	0.28
$G_{12}(Gpa)$	4.14	7.17
$S_1^T(Mpa)$	1062	1500
$S_2^T(Mpa)$	31	40
$S_{12}(Mpa)$	72	68

The results presented in Table 1 show that, for both materials considered, the burst pressure predicted by the Tsai–Wu criterion is generally higher than that predicted by the Tsai–Hill criterion. The only exceptions are $[\theta/-\theta]$ and $[\theta/-\theta]_{as}$ layups in the graphite/epoxy composite. The maximum relative difference between the predictions of the two criteria is 7.22% for graphite/epoxy and 14.7% for glass/epoxy. For both materials, the highest burst pressure is obtained with $[\theta/-\theta]_s$ layup configuration.

The variation of burst pressure with fiber angle, as predicted by the Tsai–Hill criterion, is shown in Figure 5 for several composite layups. A similar variation happens in the case of Tsai-Wu criterion. This Figure clearly shows the effect of stacking sequence on the behavior of composite laminate when the fiber angle changes. As can be seen; by using an appropriate stacking sequence and fiber angle, the burst pressure of the cylinder can be improved significantly. For the graphite/epoxy composite, the burst pressure exhibits greater sensitivity to variations in fiber angle, particularly near the optimum angle, where the rate of change is much higher.



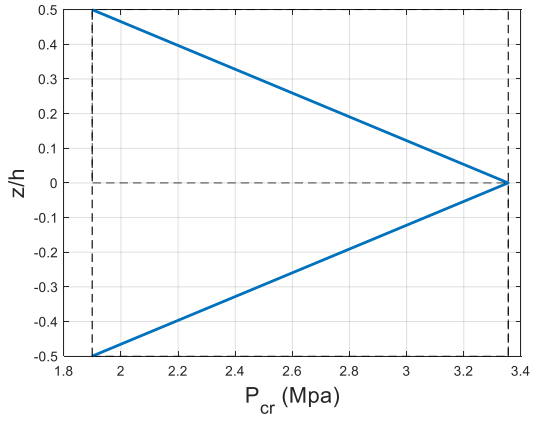
a) Graphite/epoxy



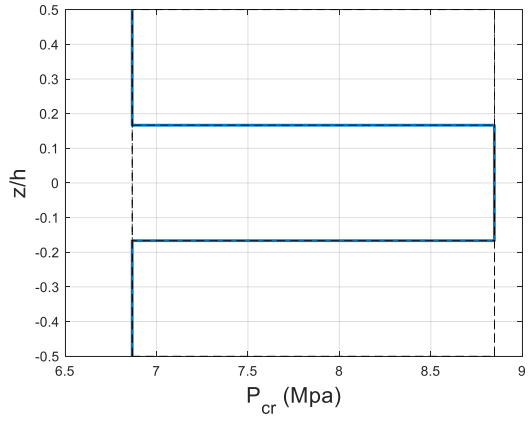
b) Glass/epoxy

Figure 5: Variation of burst pressure with fiber angle based on Tsai-Hill criterion for several composite layups.

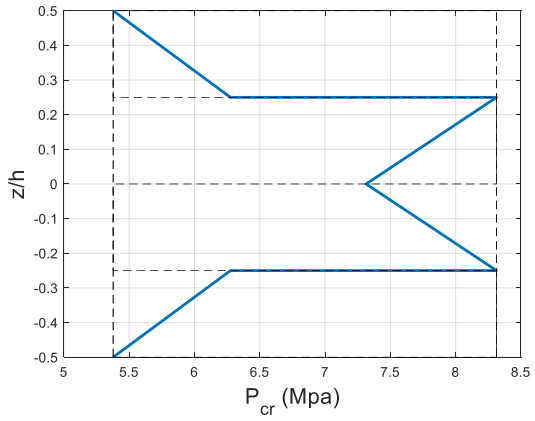
The burst pressure of a composite cylinder is governed by the stress distribution through the thickness of the laminate. Based on this stress distribution and an appropriate failure criterion, the critical pressure corresponding to each lamina surface can be determined. According to the First-Ply Failure (FPF) theory, the burst pressure is defined as the minimum of these critical pressures, indicating that failure occurs as soon as the first ply reaches its failure limit. Figure 6 illustrates the variation of the critical pressure predicted by the Tsai–Hill criterion through the laminate thickness for different stacking sequences. A similar trend is observed when the Tsai–Wu failure criterion is used.



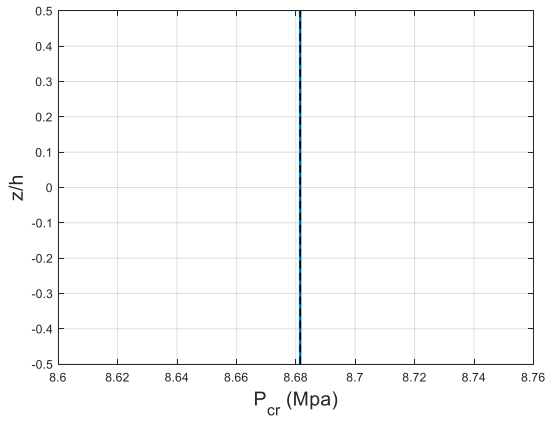
a) $[\theta/-\theta]$



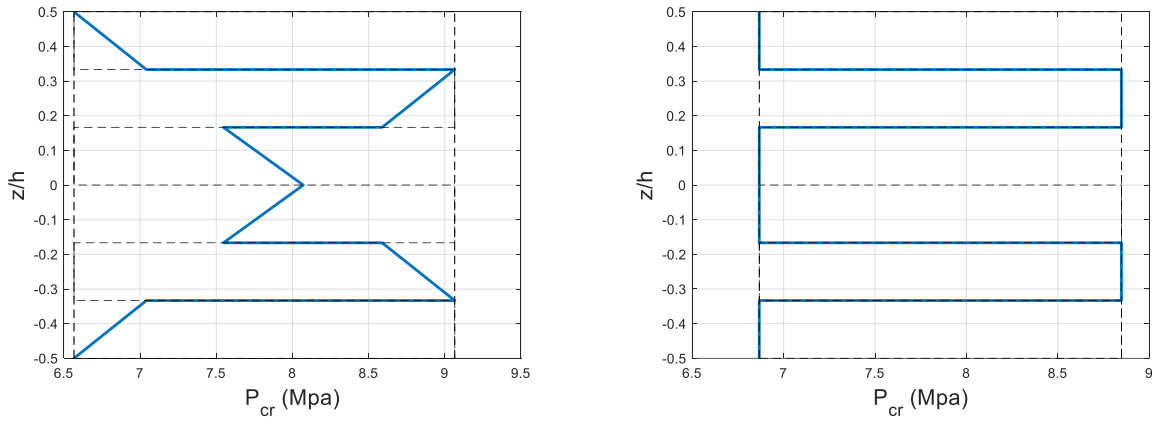
b) $[\theta/-\theta/\theta]$



c) $[\theta/-\theta]_{as}$



d) $[\theta/-\theta]_{s}$



e) $[\theta/-\theta/\theta]_{as}$ f) $[\theta/-\theta/\theta]_{s}$

Figure 6. Variation of critical pressure along the laminate thickness at the optimum fiber angle based on the Tsai–Hill criterion for graphite–epoxy composite.

According to Figure 6, failure initiates at the top and bottom surfaces of the composite for all layups. Among all the layups considered, the four-layer symmetric laminate ($[\theta/-\theta]_s$) exhibits a distinct behavior, in which the critical pressure is constant through the thickness This implies that all layers reach the burst pressure simultaneously and fail at the same time. Such behavior is considered ideal, as the full load-carrying capacity of the composite is effectively utilized. This observation is consistent with the results reported in Table 1, where this layup achieves the maximum burst pressure for both failure criteria and both materials considered.

3.3. Optimization of fiber angle and layer thickness

In this section, a multivariable optimization problem is investigated in which the fiber angle and layer thicknesses are considered as design variables. The optimization problem is solved by employing analytical sensitivity expressions relating the change of burst pressure with respect to the design variables. The results of this study are presented in Tables 3-6 for both failure criteria and for graphite/epoxy and glass/epoxy laminates. According to these Tables, for some stacking sequences (shown in bold), there is not a unique solution for thickness distribution. In these cases, there are several optimum thickness distributions that achieve the same maximum burst pressure, meaning that the optimization algorithm finds a local extremum and converges to different solutions depending on the initial guess of the design variables. To better illustrate this behavior, the variation of burst pressure with changing the thickness distribution at the optimum fiber angle is shown in Figure 7 for various stacking sequences. In this Figure, the red dots represent the maximum and

minimum burst pressures, while the black dot indicates the burst pressure corresponding to the case for which the thickness of all layers is equal. This Figure clearly demonstrates the presence of multiple peak points for some stacking sequences. This figure also indicates—based on the relative positions of the black and red dots—that, for some stacking sequences, optimizing the layer thickness distribution can lead to a significant increase in burst pressure.

Table 3: Optimum fiber angle and ply-thickness distribution for maximizing the burst pressure of the Graphite/Epoxy composite cylinder (Tsai-Hill criterion).

Lay-up	θ°_{opt}	$(t_i/h)_{opt}$	$P_{cr}\ (Mpa)$
$[\theta]$	90.00	1	1.5989
$[\theta/-\theta]$	53.67	0.5 0.5	1.8990
$[\theta/-\theta/\theta]$	53.42	0.25 0.50 0.25	8.6815
$[\theta/-\theta]_{as}$	53.42	**0.1652 0.3734 0.3348 0.1266** **0.2487 0.4975 0.2513 0.0025**	8.6815
$[\theta/-\theta]_{s}$	53.42	**0.2500 0.2500 0.2500 0.2500** **0.2500 0.3472 0.1528 0.2500**	8.6815
$[\theta/-\theta/\theta]_{as}$	53.41	**0.1113 0.2274 0.0998 0.1267 0.2889 0.1459** **0.1617 0.3658 0.1350 0.0061 0.2033 0.1281**	8.6814
$[\theta/-\theta/\theta]_{s}$	53.42	**0.0778 0.1535 0.1243 0.1243 0.3465 0.1737** **0.1164 0.2994 0.1665 0.1665 0.2006 0.0506**	8.6815
$[\theta/-\theta/0/\theta/-\theta]$	61.46	0.1446 0.3040 0.1028 0.3040 0.1446	7.5047
$[\theta/-\theta/0/-\theta/\theta]$	68.49	0.2 0.2 0.2 0.2 0.2	7.5047
$[\theta/0/-\theta]$	90.00	0.3462 0.3076 0.3462	7.5047

Table 4: Optimum fiber angle and ply-thickness distribution for maximizing the burst pressure of the Graphite/Epoxy composite cylinder (Tsai-Wu criterion).

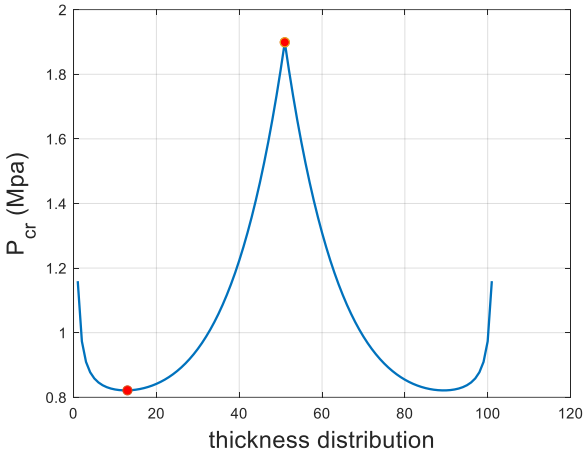
Lay-up	θ°_{opt}	$(t_i/h)_{opt}$	$P_{cr}\ (Mpa)$
$[\theta]$	90.00	1	1.6265
$[\theta/-\theta]$	54.37	0.5 0.5	1.8209
$[\theta/-\theta/\theta]$	54.19	0.25 0.50 0.25	8.9229
$[\theta/-\theta]_{as}$	54.20	**0.0977 0.3107 0.4023 0.1893** **0.1370 0.3444 0.3630 0.1556**	8.9229
$[\theta/-\theta]_{s}$	54.20	**0.2500 0.2500 0.2500 0.2500** **0.2500 0.3256 0.1744 0.2500**	8.9229
$[\theta/-\theta/\theta]_{as}$	54.20	**0.1627 0.3701 0.3357 0.0888 0.0017 0.0411** **0.1272 0.2152 0.1685 0.2192 0.2043 0.0656**	8.9229
$[\theta/-\theta/\theta]_{s}$	54.20	**0.1457 0.3174 0.1428 0.1428 0.1826 0.0686** **0.1380 0.3446 0.1801 0.1801 0.1554 0.0017**	8.9229
$[\theta/-\theta/0/\theta/-\theta]$	90.00	**0.1700 0.1761 0.3076 0.2044 0.1418** **0.3129 0.0333 0.3077 0.3430 0.0032**	8.0533
$[\theta/-\theta/0/-\theta/\theta]$	90.00	**0.3439 0.0020 0.3081 0.0020 0.3439** **0.3397 0.0065 0.3076 0.3442 0.0020**	8.0527
$[\theta/0/-\theta]$	90.00	0.3430 0.3139 0.3430	8.0458

Table 5: Optimum fiber angle and ply-thickness distribution for maximizing the burst pressure of the Glass/Epoxy composite cylinder (Tsai-Hill criterion)

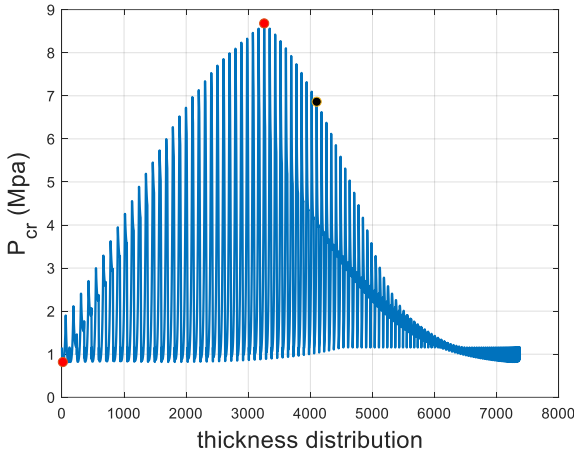
Lay-up	θ°_{opt}	$(t_i/h)_{opt}$	$P_{cr}\ (Mpa)$
$[\theta]$	90.00	1	1.2389
$[\theta/-\theta]$	90.00	0.5 0.5	1.2389
$[\theta/-\theta/\theta]$	53.69	0.25 0.50 0.25	2.3743
$[\theta/-\theta]_{as}$	53.69	**0.2487 0.4975 0.2513 0.0025** **0.1458 0.3529 0.3542 0.1471**	2.3743
$[\theta/-\theta]_{s}$	53.69	**0.2500 0.2500 0.2500 0.2500** **0.2500 0.2857 0.2143 0.2500**	2.3743
$[\theta/-\theta/\theta]_{as}$	53.68	**0.2255 0.4553 0.2729 0.0019 0.0017 0.0429** **0.0885 0.2618 0.0017 0.0421 0.4098 0.1961**	2.3743
$[\theta/-\theta/\theta]_{s}$	53.68	**0.0028 0.2506 0.2477 0.2478 0.2494 0.0017** **0.0917 0.3053 0.2032 0.2032 0.1947 0.0018**	2.3743
$[\theta/-\theta/0/\theta/-\theta]$	90.00	**0.1809 0.2097 0.2202 0.0025 0.3868** **0.3886 0.0020 0.2188 0.2196 0.1710**	2.0189
$[\theta/-\theta/0/-\theta/\theta]$	80.08	0.2012 0.2013 0.1949 0.2013 0.2013	2.0200
$[\theta/0/-\theta]$	90.00	0.3906 0.2188 0.3906	2.0200

Table 6: Optimum fiber angle and ply-thickness distribution for maximizing the burst pressure of the Glass/Epoxy composite cylinder (Tsai-Wu criterion)

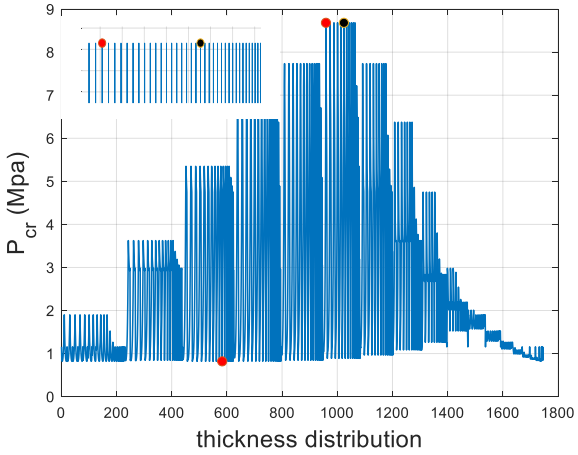
Lay-up	θ°_{opt}	$(t_i/h)_{opt}$	$P_{cr}\ (Mpa)$
$[\theta]$	90.00	1	1.3216
$[\theta/-\theta]$	90.00	0.5 0.5	1.3216
$[\theta/-\theta/\theta]$	54.22	0.25 0.50 0.25	2.7233
$[\theta/-\theta]_{as}$	54.22	**0.1298 0.3376 0.3702 0.1624** **0.0025 0.2513 0.4975 0.2487**	2.7233
$[\theta/-\theta]_{s}$	54.22	**0.2500 0.2500 0.2500 0.2500** **0.2500 0.2950 0.2050 0.2500**	2.7233
$[\theta/-\theta/\theta]_{as}$	54.19	**0.2343 0.4687 0.0017 0.0017 0.2641 0.0296** **0.0902 0.2024 0.1272 0.1488 0.2826 0.1488**	2.7233
$[\theta/-\theta/\theta]_{s}$	54.22	**0.0792 0.1306 0.1156 0.1156 0.3694 0.1896** **0.0017 0.2464 0.2448 0.2448 0.2536 0.0087**	2.7233
$[\theta/-\theta/0/\theta/-\theta]$	90.00	**0.1152 0.2754 0.2189 0.2767 0.1138** **0.3875 0.0028 0.2196 0.3878 0.0024**	2.2873
$[\theta/-\theta/0/-\theta/\theta]$	90.00	**0.1245 0.2661 0.2188 0.1900 0.2006** **0.0113 0.3793 0.2188 0.0028 0.3878**	2.2875
$[\theta/0/-\theta]$	90.00	0.3906 0.2188 0.3906	2.2874



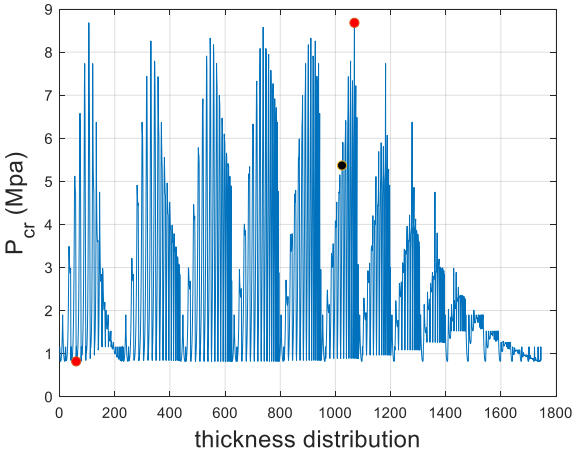
a) $[\theta\ /-\theta]$



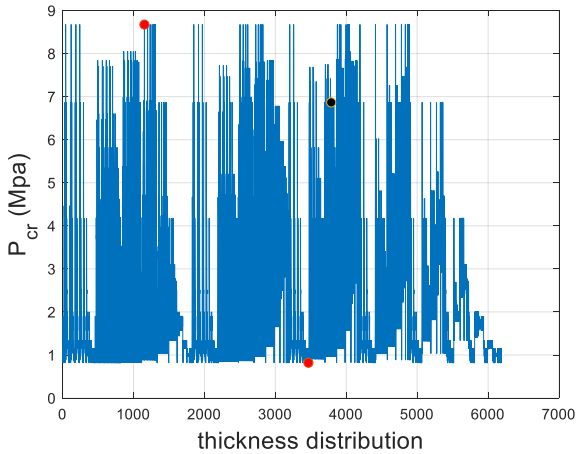
b) $[\theta/-\theta/\theta]$



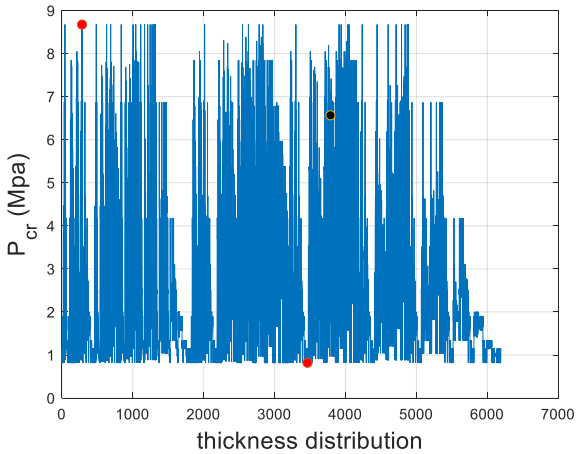
c) $[\theta/-\theta]_s$



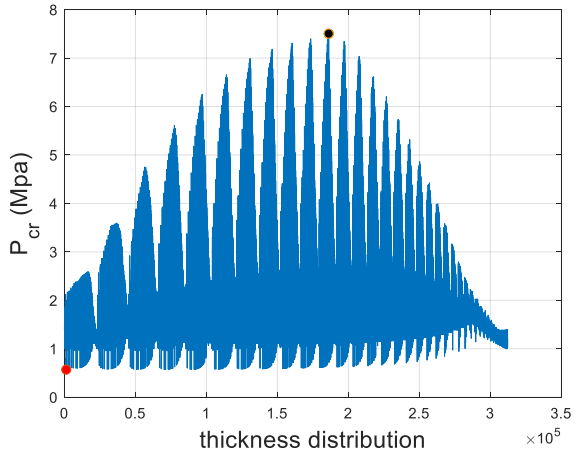
d) $[\theta/-\theta]_{as}$



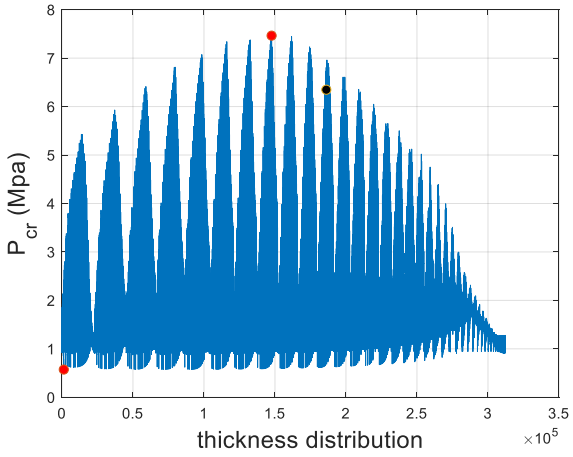
e) $[\theta/-\theta/\theta]_s$



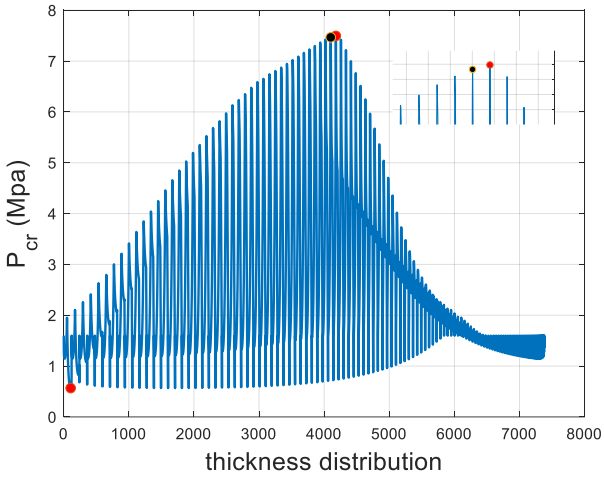
f) $[\theta/-\theta/\theta]_{as}$



g) $[\theta/-\theta/0/-\theta/\theta]$



h) $[\theta/-\theta/0/\theta/-\theta]$



i) $[\theta/0/-\theta]$

Figure 7: Variation of burst pressure with thickness distribution predicted by Tsai-Hill criterion for graphite/epoxy laminate.

The results presented in Tables 3–6 show that there is a maximum burst pressure for every stacking sequence that can be achieved by selecting appropriate fiber angle and layer thickness distribution. According to Tables 3-6, the maximum attainable burst pressure predicted by Tsai- Hill and Tsai-Wu criteria is 8.6815 Mpa and 8.9229 Mpa, respectively for graphite/epoxy laminate. These values are 2.3743 Mpa and 2.7233 Mpa for glass/epoxy laminate. In the case of laminates containing a 0° layer, the attainable maximum burst pressure in the optimized configuration decreases slightly, since this layer cannot adapt itself for best performance.

4. Conclusions

This paper investigates optimization of burst pressure in composite cylinders subjected to internal pressure. The fiber angle and thickness of layers are considered as design variables and analytical expression for sensitivity of burst pressure with respect to these variables are derived. based on the sensitivity analysis and a gradient-based optimization procedure, the optimum design variables are determined for various stacking sequences to maximize the burst pressure predicted by the Tsai–Hill and Tsai–Wu failure criteria. The obtained results indicate that the burst pressure can be significantly enhanced by appropriate selection of fiber angle and thickness distribution. Among the stacking sequences considered, the $[\theta/\ -\theta]_s$ layup shows the best performance and achieves the highest burst pressure, when only the fiber angle is optimized. The stress distribution through the laminate thickness reveals that, for this layup, all layers reach failure simultaneously, indicating an efficient utilization of the material capacity. When fiber angle and layer thickness are considered as design variables, the results show that the performance of the material can be further improved by choosing the optimum thickness distribution. The results show that each stacking sequence possesses a maximum attainable burst pressure, which can be achieved through a suitable combination of fiber angle and layer thickness distribution.

Declaration of Competing Interest

The authors declare that they have no known competing financial interests or personal relationships that could have appeared to influence the work reported in this paper.

Data availability

No data was used for the research described in the article.

Acknowledgements

No funding was received for the research described in the article.

Author contribution Saeed Abolghasemi: Data curation; Formal analysis; Investigation; Methodology; Software; Validation; Visualization; Writing – original & editing.

Funding

The author received no funding and financial support for the research, authorship, and/or publication of this article.

References

[1] Regassa Y, Gari J, Lemu HG. Composite Overwrapped Pressure Vessel Design Optimization Using Numerical Method. Journal of Composites Science. 2022;6.
[2] Shen KC, Liu XJ, Huang YH, Pan G. Strain Response and Buckling Behavior of Composite Cylindrical Shells Subjected to External Pressure with One End Fixed and the Other under Free Boundary Conditions. Sensors (Basel). 2022;22.
[3] Das SC, Paul D, Grammatikos SA, Siddiquee MAB, Papatzani S, Koralli P, et al. Effect of stacking sequence on the performance of hybrid natural/synthetic fiber reinforced polymer composite laminates. Composite Structures. 2021;276.
[4] Iwasaki KMK, Reis PA, Oliveira LG, Rauber WK, De Medeiros R. Methodology to analyse carbon fibre/epoxy composite pressure vessel based on finite element modelling and classical laminated theory. Journal of the Brazilian Society of Mechanical Sciences and Engineering. 2023;45.
[5] Neto EB, Chludzinski M, Roese P, Fonseca J, Amico S, Ferreira C. Experimental and numerical analysis of a LLDPE/HDPE liner for a composite pressure vessel. Polymer Testing. 2011;30:693-700.
[6] Chang R. Experimental and theoretical analyses of first-ply failure of laminated composite pressure vessels. Composite structures. 2000;49:237-43.
[7] Wang L, Zheng C, Luo H, Wei S, Wei Z. Continuum damage modeling and progressive failure analysis of carbon fiber/epoxy composite pressure vessel. Composite Structures. 2015;134:475-82.
[8] Rafiee R, Torabi MA. Stochastic prediction of burst pressure in composite pressure vessels. Composite Structures. 2018;185:573-83.
[9] Adali S, E. B. Summers, and V. E. Verijenko. Optimization of laminated cylindrical pressure vessels under strength criterion. Composite structures. 1993;25:305-12.
[10] Chao CC, C. T. Sun, and S. L. Koh. Strength Optimization for Cylindrical Shells of Laminated Composites. Journal of Composite Materials. 1975;9:53-66.
[11] Azeem M, Ya HH, Azad Alam M, Kumar M, Sajid Z, Gohery S, et al. Influence of winding angles on hoop stress in composite pressure vessels: Finite element analysis. Results in Engineering. 2024;21.
[12] Islam MM, Hossain MF, Rana MS, Ferdous MS. Burst pressure prediction of carbon/natural fiber and hybrid composite pressure vessels by theoretical and numerical analysis. Hybrid Advances. 2024;5.
[13] Kang C, Liu Z, Shirinzadeh B, Zhou H, Shi Y, Yu T, et al. Parametric optimization for multi-layered filament-wound cylinder based on hybrid method of GA-PSO coupled with local sensitivity analysis. Composite Structures. 2021;267.
[14] Matos H, Chaudhary B, Ngwa AN. Optimization of Composite Cylindrical Shell Structures for Hydrostatic Pressure Loading. Journal of Pressure Vessel Technology. 2023;145.
[15] Onder A, Sayman O, Dogan T, Tarakcioglu N. Burst failure load of composite pressure vessels. Composite Structures. 2009;89:159-66.
[16] Park YH, Sakai J. Optimum design of composite pressure vessel structure based on 3-dimensional failure criteria. International Journal of Material Forming. 2019;13:957-65.

[17] Shen K, Pan G. Buckling Optimization of Composite Cylinders for Underwater Vehicle Applications Under Tsai-Wu Failure Criterion Constraint. Journal of Shanghai Jiaotong University (Science). 2019;24:534-44.
[18] Xing J, Geng P, Yang T. Stress and deformation of multiple winding angle hybrid filament-wound thick cylinder under axial loading and internal and external pressure. Composite Structures. 2015;131:868-77.
[19] Zhang X, Zhao J, Wang Z. Burst Pressure Prediction and Structure Reliability Analysis of Composite Overwrapped Cylinder. Applied Composite Materials. 2017;25:1269-85.
[20] Parnas, Levend, and Nuran Katırcı. "Design of fiber-reinforced composite pressure vessels under various loading conditions." *Composite structures* 58.1 .2002; 83-95.
[21] Mian HH, Wang G, Dar UA, Zhang W. Optimization of Composite Material System and Lay-up to Achieve Minimum Weight Pressure Vessel. Applied Composite Materials. 2013;20:873-89.
[22] Liang J, Ning Z, Li Y, Gao H, Liu J, Tian W, et al. An Efficient Optimization Method for Stacking Sequence of Composite Pressure Vessels Based on Artificial Neural Network and Genetic Algorithm. Applied Composite Materials. 2024;31:959-82.
[23] Santos R, Vandepitte D, Moens D. Prediction of composite pressure vessels' burst strength through machine learning. Composite Structures. 2025;351.
[24] Jones RM. Mechanics of composite materials: CRC press; 2018.